

# EFFECT OF CHLORIDE TRANSIENTS ON CRACK GROWTH RATES IN LOW ALLOY STEELS IN BWR ENVIRONMENTS

Xiaoyuan Lou<sup>1,\*</sup> and Raj Pathania<sup>2</sup>

<sup>1</sup> GE Global Research, One Research Circle, Niskayuna, NY 12309

<sup>2</sup> Electric Power Research Institute, 3420 Hillview Ave., Palo Alto, CA 94304

## ABSTRACT

The objective of this study was to quantify the effect of chloride transients on stress corrosion cracking of pressure vessel low alloy steels. Two heats of reactor pressure vessel steel were evaluated at various chloride concentrations in both NWC and HWC environments. The tests showed that low alloy steels can exhibit a delayed cracking response during a chloride transient. The delayed response is attributed to the concentrating and dilution processes of anionic impurities inside the crack. The crack can maintain its original growth rate for a certain period after the chemistry change. The effects of chloride concentration, stress intensity factor (K) and periodic load cycling on the crack incubation and growth in low alloy steel will be discussed. The results from this work will provide a direct input to development of a crack growth model for low alloy steels, water chemistry guidelines and effects of chloride transients on crack growth.

Keywords: pressure vessel low alloy steel, stress corrosion cracking, chloride, boiling water reactor, crack growth, memory effect

## 1. INTRODUCTION

Due to the importance of reactor pressure vessel (RPV) as the key pressure boundary component in boiling water reactors (BWRs), stress corrosion cracking (SCC) of pressure vessel low alloy steel (LAS) in high temperature water has been widely studied since 1970s [1-3]. 40 years' lab and field experience has demonstrated that good practice of water chemistry in reactor can significantly reduce stress corrosion cracking susceptibility of the structural materials used in the reactor. Three chemistry action levels have been established in EPRI boiling water reactor water chemistry guideline [4] with increasing order of severity. Action levels were determined based on quantitative analysis on the effects of the chemistry variables on the corrosion behavior of reactor materials, fuel performance and radiation field buildup. For chloride transient in primary cooling water, Table 1 shows the 2014 guideline for chloride levels. The lowest action level of chloride was  $\geq 5$  ppb for both NWC and HWC in the 2014 guideline.

However, independent work conducted in Paul Scherrer Institute (PSI) and GE confirmed a very pronounced effect of chloride, at levels as low as 3 ppb, in initiating and sustaining rapid crack growth in low alloy steel [5-9]. Therefore, based on the results of these studies BWRVIP issued an Interim Guidance in 2016 revising the chloride action limit to  $\geq 3$ ppb.

The new observations of SCC susceptibility of pressure vessel steel at  $< 5$  ppb chloride raised a concern for the current fleet of boiling water reactors. Chloride can be introduced into the reactor cooling system during periods of significant condenser in-leakage or other incidents. To determine the impact of this period on the existing flaws on pressure vessel steel, it is critical to obtain the crack growth rate data of the steel in chloride containing environments and understand how long the fast growth rate can sustain after the clean-up. GE has observed that low alloy steels can exhibit a delayed cracking response under the transient of chloride. There is an incubation time before the crack growth rate starts to increase after chloride is added. Similarly, there is a delay time or so called "memory" effect after chloride is removed before the crack growth rate starts to decrease. These observations raised concerns in regard of the evaluation of crack growth rates in the primary pressure boundary components after the chloride transient. The adequacy of the current BWRVIP-60-A stress corrosion cracking (SCC) disposition lines (DLs) need to be re-evaluated for chloride transient conditions.

\* Currently with CorroMet LLC

The main purpose of this research was to generate data to support the possible revision of BWRVIP-60-A LAS SCC disposition lines for chloride transient. Quantitative analysis of memory effects is also conducted to determine impact of chemical transient and operation practice during the transient. Two different heats of pressure vessel steel from the actual reactor pressure vessels (RPV) were evaluated under both periodic partial unloading (PPU) condition and constant load/K condition without unloading. A wide range of chloride levels (5 ppb, 20 ppb, 100 ppb, 500 ppb for NWC, and 5 ppb, 50 ppb, 200 ppb, 500 ppb for HWC) were evaluated to provide adequate data to all three action levels and possible severe condition beyond the action level 3. Effects of electrochemical potential (ECP), stress intensity factor (K), and heat-to-heat difference were also studied in detail.

## 2. EXPERIMENTAL PROCEDURES

Two different heats of high sulfur low alloy steels were tested in this study. Table 2 shows the chemical compositions of the steels. Both heats were studied in the previous EPRI-GE program for evaluating the impact of <5 ppb chloride on SCC of LAS in high temperature water [7]. SWRI heat is A533 Grade B Class 1 LAS from the reactor pressure vessel head of a canceled plant. Figure 1 shows the orientation of the material relative to the vessel heat plate. This heat has been used in EPRI's RPV boric acid corrosion testing program. 1bG heat is also A533B grade LAS, and this specific heat was used in a previous BWRVIP test program. Both materials were tested along T-S orientation in this study to simulate through-wall crack propagation in the reactor vessel.

Since all the materials received were from the actual reactor vessels, they were tested in as-received condition with no additional treatment. The crack growth rate tests were performed using 1-inch (1T) compact tension (CT) specimens with 5% side grooves on each side. The tests were conducted in 288 °C BWR water. A close-loop system with demineralizer was used to purify the outlet water from the autoclave back to above 18 MΩ-cm. Chloride concentration in the autoclave was maintained by injecting the dilute HCl solution and controlling the water inlet conductivity to a pre-calculated constant value. The study was conducted in both, low corrosion potential hydrogenated water (63 ppb H<sub>2</sub> in water) and high corrosion potential oxygenated water (2 ppm O<sub>2</sub>). The CT specimens were instrumented with platinum current and potential leads for dc potential drop (DCPD) measurements of crack length. Current flow through the specimen was reversed about once per second to reduce the measurement errors associated with thermocouple effects and amplifier offsets. A DCPD correction factor must be accurately estimated to ensure little or no rise in K during the exposure period. The final crack growth rate was also calculated based on the fracture micrograph performed after the test. The computer controlled current reversal, data acquisition, data averaging, the calculation of crack length from the potential, and the auto-control of constant stress intensity factor (K). [10, 11] The specimen was electrically insulated from the loading rig by zirconia sleeve and washer. Within the autoclave a zirconia washer also isolated the upper pull rod from the internal load frame. The lower pull rod was electrically isolated from the autoclave using a pressure seal and an insulating washer. Fatigue pre-cracking was performed at the beginning of each test at ~1 Hz and an increasing load ratio ( $K_{min}/K_{max}$ ) R = 0.2, 0.4, and 0.6. Subsequent pre-crack steps to transition the crack to intergranular type were performed by decreasing the frequency to 0.001 Hz, then by introducing a hold time, and finally to a fully constant K test with no cycling. The corrosion potentials of the CT specimen and a Pt coupon were measured relative to a zirconia membrane Cu/CuO reference electrode. [12]

The main focus was generating stress corrosion crack growth rate data to re-evaluate the SCC behaviors of low alloy steel at different chloride transient conditions. SCC memory effects was quantified by evaluating the delayed time of the cracking response to a change in chloride concentration (both chloride increase and decrease). Figure 2 shows the schematic of both time-to-activation and time-to-arrest of a stress corrosion cracking during a chloride transient. Time-to-activation defines the incubation time before the crack growth rate starts to increase after chloride is added, while time-to-arrest defines a so called "memory" effect after chloride is removed before the crack growth rate starts to decrease.

### 3. RESULTS

#### 3.1 Crack growth rate under constant load in normal water chemistry

Figure 3 shows a summary of crack growth rate data from both SWRI and 1bG heats under constant load/K condition and different chloride levels. The data are plotted against EPRI BWRVIP-60-A LAS SCC disposition line, also to GE low and high sulfur lines. In all these tests, the loading conditions did not exceed the K/size criteria by ASTM E399. Those SCC growth tests which did not show sustained crack growth were not included in this plot. It should be kept in mind that there were still data showing no crack growth that are not included in Figure 3. The data at <5ppb chloride condition was obtained from earlier research [7] and tested in higher oxygen conditions (8 ppb). With the chloride transient at 5 ppb–100 ppb, most stress corrosion cracks exhibited growth rate higher than GE low sulfur line. But all the cracks were still bounded by GE high sulfur line. Generally speaking, stress corrosion crack growth rate in low alloy steel increases as K and chloride increase. The only data showing the crack growth rate above high sulfur line was during the chloride transient of 500 ppb. But when the chloride level is above 100 ppb, the chemistry reaches action level 3 (Table 1) and the reactor should be shut down. With SWRI heat and 1bG heat, there were few data showing high crack growth rate when the chloride was below 5 ppb. But according to our previous research [7], on a more susceptible heat of low alloy steel from a plant (PSI heat), 3–5 ppb chloride can activate an arrested crack and sustain the high crack growth rate when the corrosion potential is very high.

#### 3.2 Crack growth rate under constant load in hydrogenated water chemistry

Figure 4 shows a summary of SCC crack growth rate of both SWRI and 1bG steels in hydrogenated water containing 63 ppb H<sub>2</sub>. The chloride levels used in this study were 5 ppb, 50 ppb, 200 ppb, and 500 ppb. It should be noted that a chloride concentration of 50 ppb exceeds Action Level 2 and 200–500 ppb chloride exceeds Action Level 3. The purpose of testing at these high concentrations was to evaluate the effect of severe chloride transients on crack growth rates. Such transients can occur in plants because of condenser tube failures. Under constant load/K condition where K is in a range of 49.5–55 MPa√m, stress corrosion cracks in both heats show no growth in hydrogenated water. Under cyclic load condition at R = 0.6 and Frequency = 0.001Hz, cracks can sustain the growth. However, no chloride effect was observed in all the tests in HWC at the chloride level up to 500 ppb. Therefore, in HWC, low alloy steel shows no SCC risk during a chloride transient up to 500 ppb in this research.

#### 3.3 Heat-to-heat Comparison

Figures 5 and 6 show the comparison of crack growth rate of two different LAS heats tested in this program in two different chloride conditions (20 ppb Cl and 100 ppb Cl). The tests showed that there was no apparent difference in SCC growth rate in these two heats of pressure vessel steels in BWR normal water chemistry. Though some cracks exhibited slow crack growth rates in the plots, most cracks showed high growth rates and the data from two heats overlapped on each other. SCC susceptibility of both heats increases as K and chloride increases. Earlier work on these two heats has shown that SWRI and 1bG heats have similar chemical composition, sulfide distribution, and grain structure. This result is consistent with the earlier observations [7].

#### 3.4 Chloride memory effect on stress corrosion crack of low alloy steel

Figure 7 shows how a stress corrosion crack in low alloy steel responds to chloride incubation and memory effect during and after the chloride transient. The behavior of a stress corrosion crack can be described in 4 different steps during a chloride transient period, as listed below:

- 1) Time-to-activation: the time period that is needed to re-activate an arrested crack. This delayed response may be attributed to the transport of the anions through the crack and oxide to the crack tip.

- 2) Crack growth period: fast crack growth in chloride containing environment after the crack activation.
- 3) Chloride clean-up period: the time that is taken to clean the reactor water.
- 4) Time-to-arrest: the time that is needed to arrest the growing crack in pure water.

This paper defines the starting time of time-to-activation by the time when the reactor water reaches the targeted chloride level. In the same way, the starting time of time-to-arrest is defined by the moment when the reactor water reaches  $< 1$  ppb Cl. The ending time of time-to-arrest in this research is defined by the moment when the crack growth rate is below  $3 \times 10^{-7}$  mm/s.

With the 4-liter autoclave set-up in GE lab, the water clean-up usually takes about 4 hours. Most of the data obtained in this program show that the crack generally does not slow down during the chloride clean-up period. It is reasonable to treat the crack during the clean-up period with the same growth rate as it does in chloride containing water. However, after the clean-up period, the crack can keep the same fast growth rate for a while. It should be noted that the fast momentum of the crack generally does not take long. Although it can take very long time to fully arrest a crack from chloride transient, the advance of a crack in low alloy steel is in general slow for the most of the time.

Figure 8 shows the summary of time-to-activate when the chloride level in reactor increases to the action level. The plot only includes the crack that could be activated in the test. There were many cases where the arrested crack could not be re-activated within 300-500 hours of testing time in this study. The data in  $< 5$  ppb chloride from the earlier research program (different heat and 8 ppm  $O_2$  condition) is also included for comparison. From these data, it is not so clear to conclude how the time-to-activation during a chloride transient is related to both chloride level and K level. The large variation in time-to-activation may be due to the variation in the starting status of a crack (crack length, crack front evenness, oxide inside crack, crack tip bluntness, etc.) The maximum time-to-activation was around 250 hour, which does not include those cracks that could not be activated. Though there were a few cracks that required very long time to activate, most cracks could be activated within 70 hours.

Figure 9 summarizes how long it takes to arrest an actively growing crack after the chloride contamination was cleaned from the reactor cooling water. The time-to-arrest in the paper only counts the time when the crack growth rate was higher than  $3 \times 10^{-7}$  mm/s. It is true that cracks may take long time to be fully arrested (crack growth rate is equal to zero). But we should not take too much consideration of the period when the crack grew slowly due to the following reasons: (1) the crack advance in length during this period was generally very small even though the time was long; (2) there can be huge variations if counting the arrest time of a slowly growing crack, which can provide misleading conclusions on how the arresting crack will impact the reactor pressure vessel. In most cases, such information tends to overestimate the damage to the reactor vessel. Though the data were scattered, the plot still shows the trend that time-to-arrest of a growing crack after chloride clean-up increased as the chloride level and K increased. The maximum time-to-activation was around 50 hours. By comparing Figure 9 with Figure 8, it can be concluded that the time-to-arrest was generally less than the time-to-activation in all tested K and chloride levels. Based on the data in this study, it may not be necessary to have a penalty on the vessel life assessment because of the memory effect of the chloride clean-up because it will be balanced by the time to crack activation.

While the delayed time can provide some insights to how to quantify chloride memory, it is also important to understand how deep the crack can actually grow during this period so people can better assess the actual damage created by the memory effect after the chloride clean-up. Figure 10 shows the summary of the crack advance length measured from CT specimens after the chloride clean-up. Different from time-to-arrest, those data were obtained by calculating the time between the moment when water reached zero chloride condition and the moment when the crack was fully arrested (no growth). In all the tested heats and conditions, there was only one crack that grew for around 0.62mm before it fully stopped. Most data show the crack extension after the water clean-up was below 0.3-0.4 mm in NWC. It is interesting to note

that no clear correlation was observed between the actual crack extension and the chloride/K levels. All the arresting cracks in different chloride and K conditions grew similar distances after the chloride clean-up.

#### **4. CONCLUSIONS**

SCC crack growth rates of pressure vessel low alloy steel were evaluated at 288 °C with 5, 20, 100, and 500 ppb chloride for normal water chemistry (NWC) and 5, 50, 200, and 500 ppb chloride for hydrogen water chemistry (HWC). The study also quantitatively evaluates the impact from the delayed cracking response during chloride transient (so-called memory effect) to the existing flaw in the pressure vessel steel. In NWC, higher chloride level increases the crack growth rate of LAS. GE low sulfur line cannot bound the crack growth rate data at >3ppb chloride. However, GE high sulfur line is still a good bound for all the tested CGRs up to action level 3 (100 ppb chloride). In hydrogen water chemistry, no chloride effect or chloride memory effect was observed in all the tested heats and chloride/K conditions in this study. The crack arrest generally takes less time than crack activation during chloride transient period in all tested K and chloride levels. Based on the data analysis in this study, it may not be necessary to put a penalty on the vessel life assessment due to the impact from the memory effect of the chloride clean-up because it will be balanced by the effect of time to crack activation.

#### **ACKNOWLEDGMENTS**

This research is sponsored by Boiling Water Reactor Vessel and Internals Program, Electric Power Research Institute. Authors thank Dr. Peter Andresen for many helpful discussion.

#### **REFERENCES**

- [1] P.L. Andresen, L.M. Young, Crack Tip Microsampling and Growth Rate Measurements in Low Alloy Steel in High Temperature Water, *Corrosion*, 51 (1995) 223.
- [2] F.P. Ford, P.L. Andresen, Stress Corrosion Cracking of Low Alloy Steels in 288C Water, NACE, New Orleans, 1989.
- [3] F.P. Ford, D.F. Taylor, P.L. Andresen, R.G. Ballinger, Environmentally-controlled cracking of stainless and low-alloy steels in light-water reactor environments, 2006.
- [4] EPRI, BWRVIP-190 Revision 1: BWR Vessel and Internals Project, Volume 1: BWR Water Chemistry Guidelines - Mandatory, Needed, and Good Practice Guidance, EPRI, Palo Alto, CA, 2014.
- [5] H.P. Seifert, S. Ritter, Research and service experience with environmentally-assisted cracking of carbon and low-alloy steels in high-temperature water, Stockholm, Sweden, 2006.
- [6] H.P. Seifert, S. Ritter, The influence of ppb levels of chloride impurities on the stress corrosion crack growth behaviour of low-alloy steels under simulated boiling water reactor conditions, *Corros. Sci.*, 108 (2016) 134-147.
- [7] X.Y. Lou, P.L. Andresen, BWRVIP-292: Effects of Low Level Chloride on Stress Corrosion Cracking of Low Alloy Pressure Vessel Steels in BWR Environments, 3002005622, EPRI, Palo Alto, CA, USA, 2015.

- [8] X.Y. Lou, P.L. Andresen, T.G. Lian, R. Pathania, Effect of ppb levels of chloride on the stress corrosion cracking of pressure vessel steel, Canadian Nuclear Society, Ottawa, Ontario, Canada, 2015.
- [9] H.P. Seifert, S. Ritter, Stress corrosion cracking of low-alloy reactor pressure vessel steels under boiling water reactor conditions, *J. Nucl. Mater.*, 372 (2008) 114-131.
- [10] P.L. Andresen, C.L. Briant, Environmentally assisted cracking of types 304L/316L/316NG stainless steel in 288C water, *Corrosion*, 45 (1989) 448-463.
- [11] P.L. Andresen, Environmentally assisted growth rate response of nonsensitized AISI 316 grade stainless steels in high temperature water, *Corrosion*, 44 (1988) 450.
- [12] L.W. Niedrach, A new membrane type pH sensor for use in high temperature high pressure water, *J. Electrochem. Soc.*, 127 (1980) 2122.
- [13] C. Marks, D. Macdonald, W. Coulson, Materials Reliability Program Reactor Vessel Head Boric Acid Corrosion Testing (MRP-165), Electric Power Research Institute, Palo Alto, 2005.

## TABLES

Table 1. EPRI boiling water reactor water chemistry control guideline for NWC, HWC and HWC+NMCA or OLNC (data from [4])

	<b>Action Level 1</b>	<b>Action Level 2</b>	<b>Action Level 3</b>
<b>Chloride</b>	≥5 ppb	>20 ppb	>100 ppb
<b>Sulfate</b>	>5 ppb	>20 ppb	>100 ppb

Table 2. Chemical compositions of the steels tested (wt%)

	<b>S</b>	<b>C</b>	<b>Al</b>	<b>Co</b>	<b>Cr</b>	<b>Cu</b>	<b>Mn</b>	<b>Mo</b>	<b>Ni</b>	<b>Si</b>	<b>P</b>	<b>V</b>
<b>SWRI</b>	<b>0.015</b>	<b>0.2</b>	<b>0.021</b>	<b>0.018</b>	<b>0.066</b>	<b>0.07</b>	<b>1.25</b>	<b>0.55</b>	<b>0.58</b>	<b>0.23</b>	<b>0.01</b>	<b>0.0015</b>
<b>1bG</b>	<b>0.013</b>	<b>0.19</b>	<b>0.028</b>	<b>0.017</b>	<b>0.078</b>	<b>0.099</b>	<b>1.25</b>	<b>0.53</b>	<b>0.62</b>	<b>0.25</b>	<b>0.01</b>	<b>0.003</b>

## FIGURES

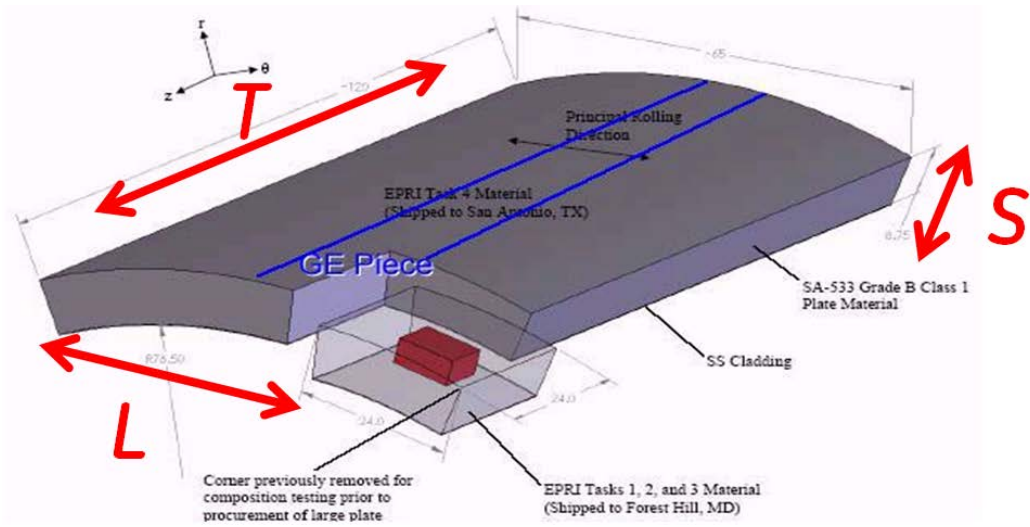
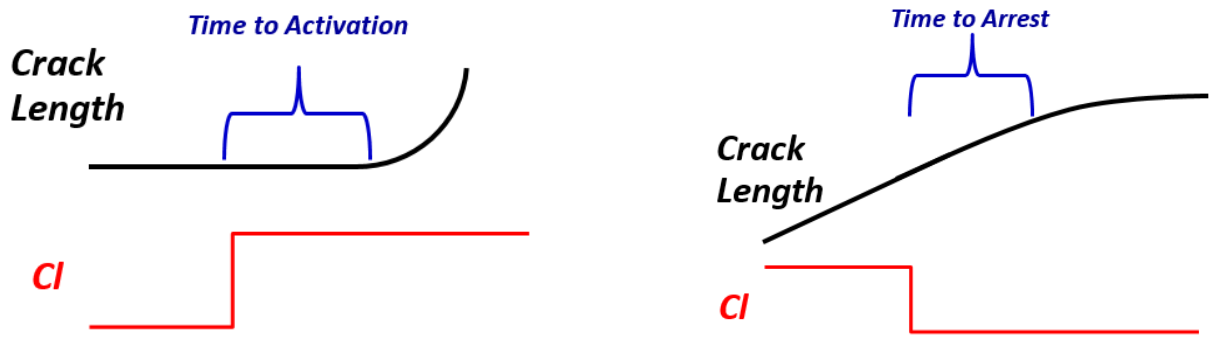


Figure 1. Specimen orientation relative to the vessel plate sent to GE (re-plotted based on reference [13])



(a) Time to activation after chloride increase

(b) Time to arrest after chloride decrease

Figure 2. Schematic of the definition of stress corrosion crack memory in this report



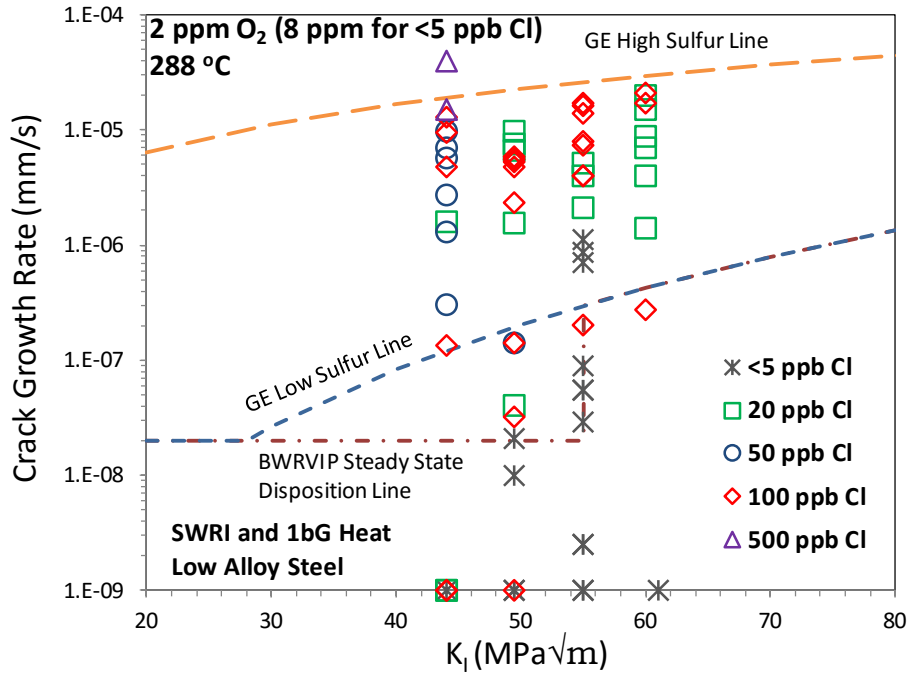


Figure 3. Summary of the crack growth rates measured under constant load/K condition in this program compared with BWRVIP/GE disposition lines

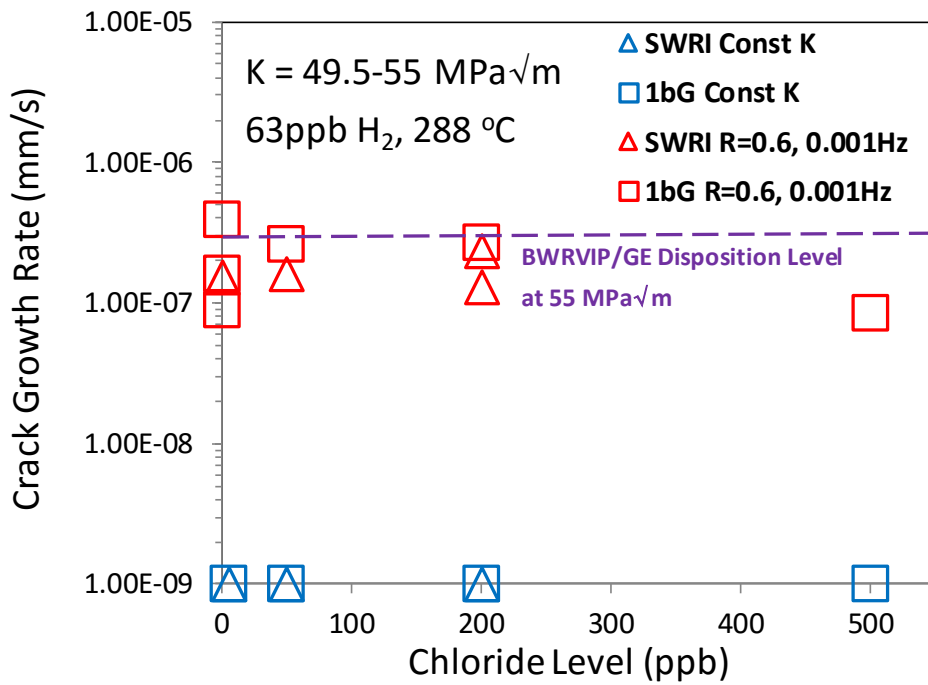


Figure 4. Summary of CGRs in 63 ppb hydrogenated water at  $K= 49.5-55$  MPa√m under both constant load and cyclic load conditions

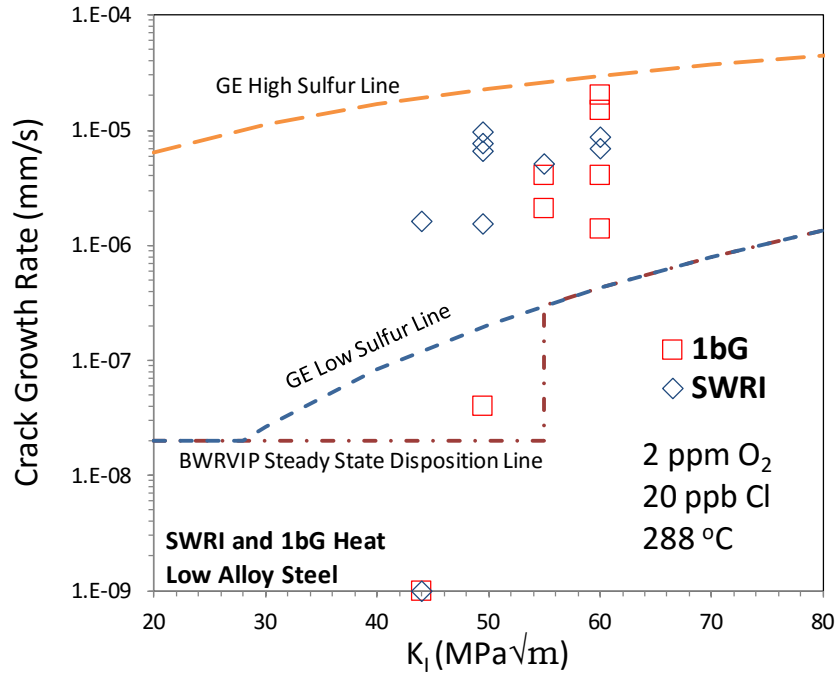


Figure 5. Comparison of crack growth rate of two different heats at 2 ppm  $O_2$  and 20 ppb Cl

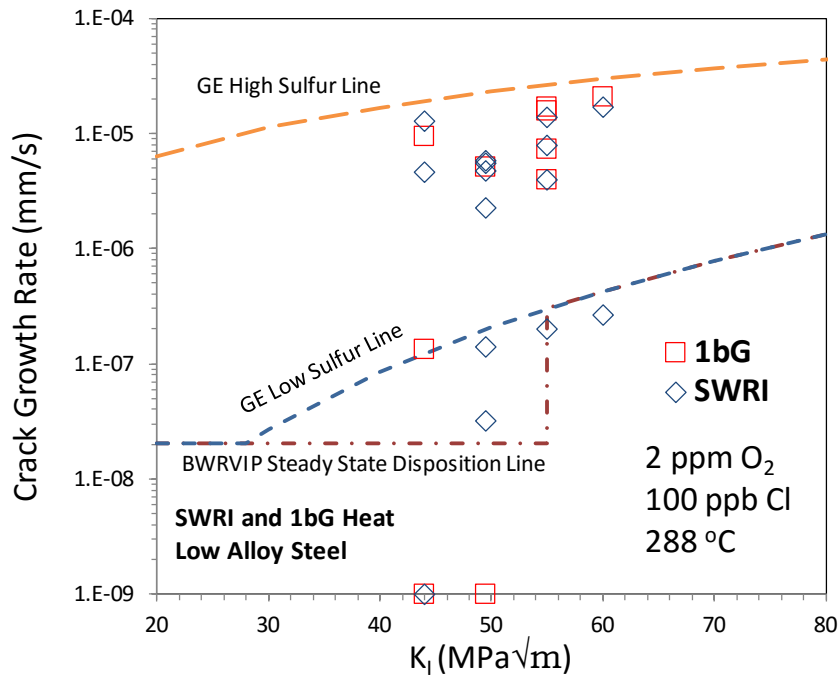


Figure 6. Comparison of crack growth rate of two different heats at 2 ppm  $O_2$  and 100 ppb Cl

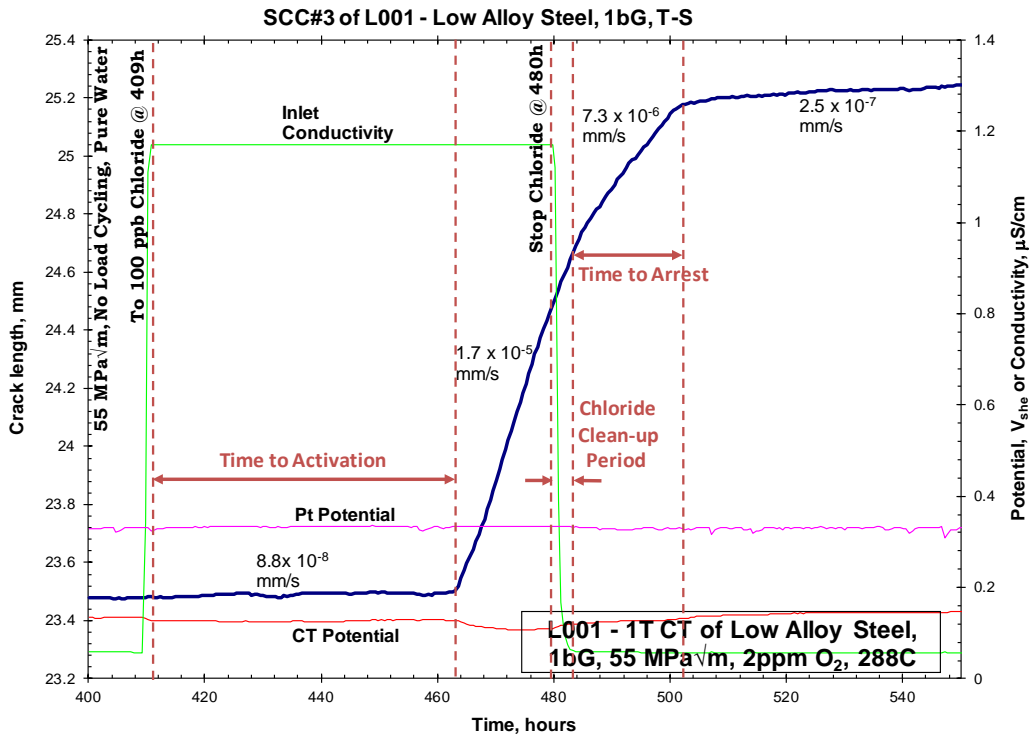


Figure 7. A typical example of chloride memory effect in low alloy steel

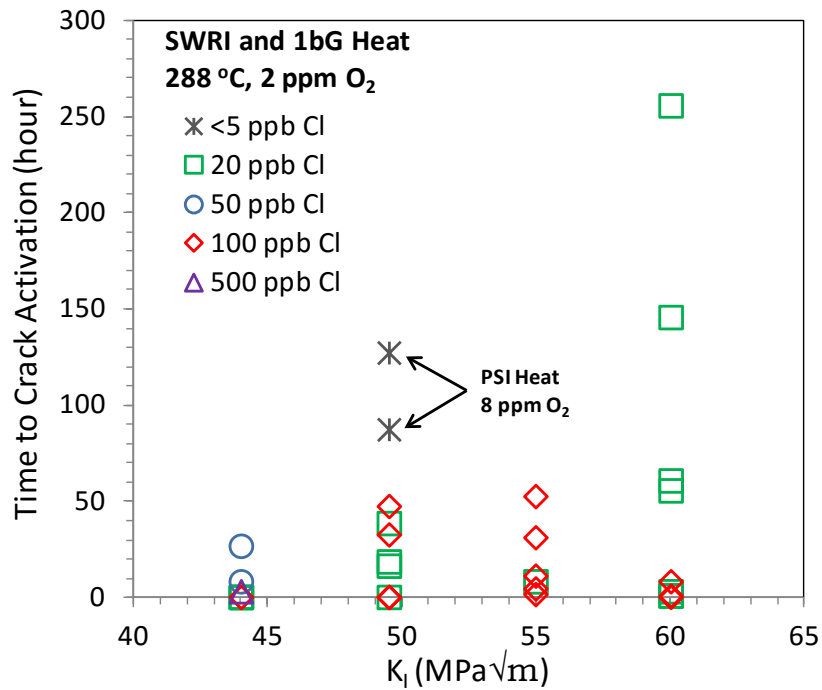


Figure 8. Summary of time-to-activation during the chloride transient

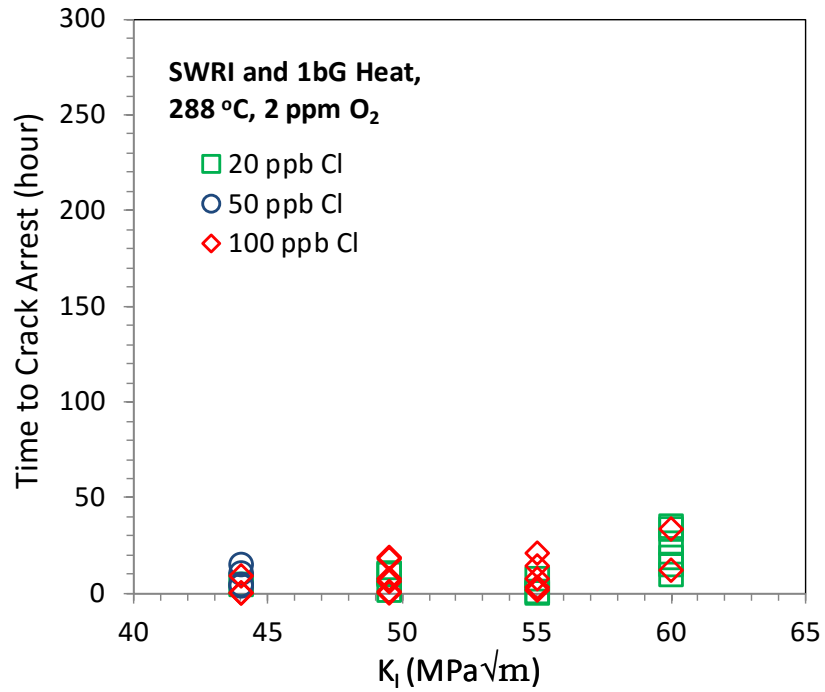


Figure 9. Summary of time-to-arrest after the chloride clean-up

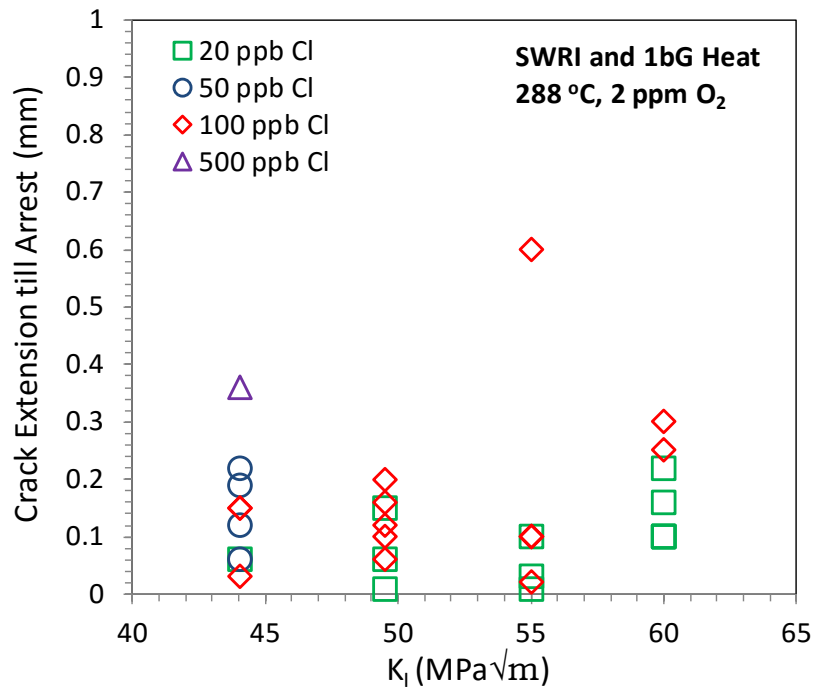


Figure 10. Crack extension after the chloride clean-up (data was obtained by calculating the time between the moment when water reached zero chloride condition and the moment when the crack was fully arrested (no growth))